



# Experimental and Numerical Analysis on the Stress Performance of Steel Plate-Concrete Combination Wall of Assembled Underground Silo

Hao Zhang, Kang Yang, Lei Chen\*, Hongkai Wang, Kaiyi Han, Lingling Yuan

College of Civil Engineering, Henan University of Technology, Zhengzhou 450001, China

\*Email address: ayk666666@163.com, Telephone number: 15565475771

**Abstract.** As a new type of storage structure, the prefabricated steel plate-concrete underground silo can efficiently utilize underground space, save energy and reduce carbon emissions, and ensure a sealed low-temperature grain storage environment. The analysis of internal forces and displacements of the composite silo wall is one of the key technical issues that need to be addressed in the design of underground silos. This study adopts a combination of experimental and numerical simulation methods to analyze the mechanical properties of the silo wall under the most unfavorable working condition (empty silo) soil pressure load; it explores the influence of concrete strength, external waterproof steel plate thickness, and internal steel plate thickness on the stress and displacement of the silo wall. The results show that under the soil pressure load, the circumferential stress at the same height of a single silo wall varies little, with smaller values on both sides of the wall and larger values in the middle. The numerical analysis results are in good agreement with the experimental results, where the average errors between the experimental and simulated values of the circumferential stress of the internal steel plate and the circumferential reinforcement of the silo wall are 7.84% and 6.56%, respectively. Within the selected parameter range, concrete strength and internal steel plate thickness have a significant impact on the circumferential stress of the internal steel plate of the silo wall and the radial displacement of the silo wall, and suggestions for selecting parameters are provided. This study can provide a reference for the engineering design of steel plate-concrete underground silos.

**Keywords:** assembled underground silo; full-scale test; mechanical performance; parameter analysis

## 1 Introduction

The storage of grain is of profound significance for safeguarding national food security, promoting the stable and healthy development of the economy, and enhancing the country's overall risk resistance capabilities<sup>[1]</sup>. Existing types of grain storage facilities, such as flat warehouses, shallow circular silos, and vertical silos, all have their respective

shortcomings and are susceptible to environmental factors such as temperature, humidity, pests, and mold. The underground silos has a long history<sup>[2-3]</sup>. Compared with traditional grain storage structures, the prefabricated underground grain silo can effectively utilize underground space for grain storage. The naturally low temperature of the underground grain silo can significantly reduce the need for cooling measures, thereby saving a substantial amount of electricity used by refrigeration equipment and conserving energy. Moreover, grain quality is more easily ensured. Wang Zhenqing et al.<sup>[4]</sup> summarized the development process and current status of underground silo structural design in China, proposed a new design scheme using prefabricated and composite structural technologies, and conducted a comparative analysis of the advantages and disadvantages of different structural forms. They emphasized the significant research and application value of the new type of underground silo in the grain storage industry.

Currently, scholars have conducted research on the cast-in-place reinforced concrete underground silos, achieving significant results especially in aspects such as pit support<sup>[5]</sup> and structural anti-floating<sup>[6,7]</sup>. However, challenges still remain, including the high-standard waterproofing and moisture-proofing of the silo body, reliable node connections of the silo walls, and research on the overall structural load-bearing behavior. Regarding the waterproofing of the silo body, Zhang Hao et al.<sup>[8-11]</sup> proposed a polypropylene–concrete silo wall waterproofing system. They designed test specimens of polypropylene plastic liner–concrete silo walls and investigated their failure modes, internal force changes, and water pressure–bearing capacity. To address the node connection problem of the silo walls, Wang Zhenqing, Zhang Hao et al.<sup>[12-14]</sup> proposed various connection forms for the prefabricated steel plate–concrete underground silos and conducted mechanical property tests on the nodes, proving that these nodes have high load-bearing capacity and can provide safe and reliable connections for the silo walls. For the internal force calculation of underground silos, Kim et al.<sup>[15, 16]</sup> performed numerical analyses by establishing three-dimensional finite element models of cast-in-place reinforced concrete underground silos. They evaluated the load-bearing capacity and stress state of the structure under different lateral pressure coefficients and verified that the structure is within the allowable stress range of the design and has sufficient safety.

For prefabricated underground silos, research on the load-bearing characteristics of the silo walls is still limited. This study, based on the first domestic prefabricated steel plate–concrete underground grain silo project, employs a combination of experimental and numerical simulation methods to investigate the distribution patterns of the circumferential stress of the underground silo walls. It also explores the influence of concrete strength, external waterproof steel plate thickness, and internal steel plate thickness on the stress and displacement of the silo walls, providing references for relevant engineering design.

## 2 Experimental Study

### 2.1 Project Overview

This study takes an actual prefabricated steel plate–concrete composite underground silo project as the research object. The total depth of the silo is 24.5 m, with an inner diameter of 25 m and a wall thickness of 310 mm, including a 10-mm-thick steel liner and a 300-mm-thick layer of concrete, as shown in Fig.1. The roof and floor of the silo are cast-in-place steel plate–concrete composite structures, while the silo walls are assembled from prefabricated steel plate–concrete composite components. The entire circumference of the silo wall is composed of 12 wall segments, which are connected by steel plate welding to form the joints, the details of which are illustrated in the figure. The silo walls are assembled in three vertical layers. The entire underground grain silo structure uses steel grade Q355B, concrete grade C40, and rebar grade HRB400.



Note: The yellow dot indicates the prefabricated module of measuring point layout.

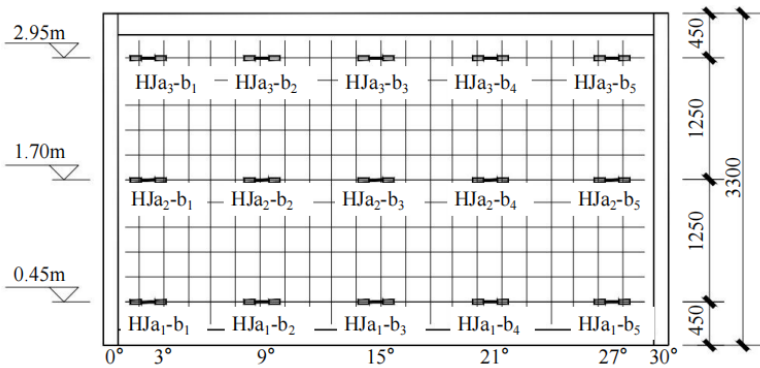
**Fig. 1.** Site construction diagram of assembled underground silo.

### 2.2 Layout of Measuring Points

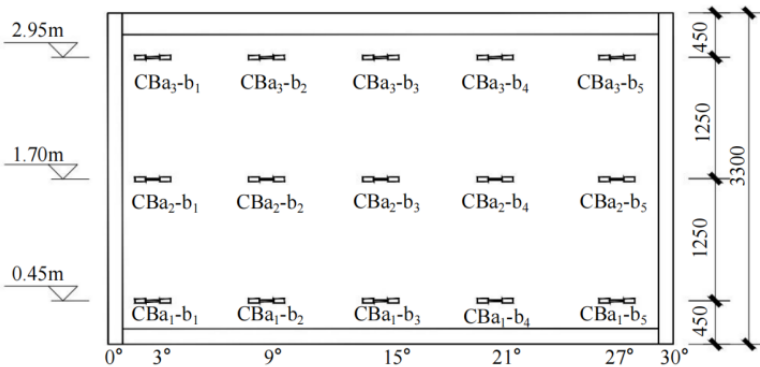
To investigate the distribution pattern of the circumferential stress in the silo wall, strain gauges were pre-embedded in the silo wall before the casting of the wall in the prefabrication plant. The distribution of the reinforcement bar mesh in the wall of the lowermost ring of the underground silo (indicated by the yellow dots in Fig.1) was equipped with vibrating wire rebar strain gauges to monitor the variation pattern of the circumferential stress in the hoop reinforcement. As shown in Fig.2a, each measurement point is denoted by  $HJ_{a_i-b_j}$ , where  $a_i$  represents the vertical measurement points. There are three layers from bottom to top, representing the points at heights of 0.45 m, 1.70 m, and 2.95 m (calculated with the bottom of the lowermost ring of the silo wall as  $\pm 0.00$

m), labeled as  $a_1$ - $a_3$ . The symbol  $b_j$  indicates the measurement points arranged along the circumferential direction of a single prefabricated block, with five points from left to right labeled as  $b_1$ - $b_5$ . For example,  $HJa_1$ - $b_1$  represents the first measurement point from left to right along the circumferential direction at a height of 0.45 m in the prefabricated silo wall. On the same silo wall, vibrating wire rebar strain gauges were arranged on the contact surface between the internal steel plate and the concrete to measure the variation pattern of the circumferential stress in the internal steel plate under the action of earth pressure. The numbering rule is the same as that for the hoop reinforcement measurement points, that is,  $CBa_1$ - $b_1$  to  $CBa_5$ - $b_3$ , as shown in Fig.2b.

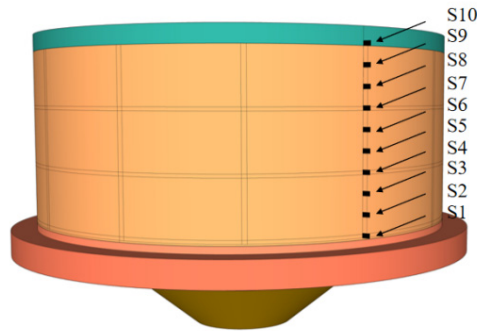
To measure the water and earth pressure acting on the external surface of the composite silo wall during backfilling, earth pressure cells were installed along the height direction of the external waterproof steel plate on the right side of the prefabricated block of the silo wall. A total of 10 earth pressure cells were installed, with one cell every 1.1m from the bottom of the lowermost ring of the silo wall to the top of the uppermost ring, and they were numbered from bottom to top as S1-S10, as shown in Fig.2c.



a. Layout of ring reinforcement measuring points.



b. Layout of internal steel plate measuring points.



c. Layout of measuring points of earth pressure gauge.

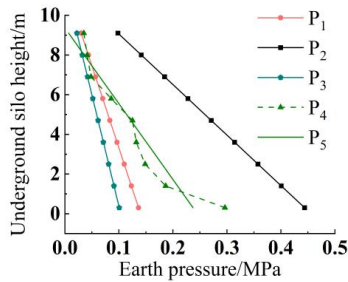
**Fig. 2.** Layout of underground silo measurement points

### 2.3 Analysis of Test Results

Following the completion of the main structure construction of the underground silo, soil backfilling was carried out, with the maximum backfill height reaching 12.4 m (the top of the uppermost ring of the silo wall). When the backfill height reached 12.4 m, the earth pressure load had the most adverse effect on the internal forces of the silo wall. As shown in Fig.3a, with the increase in the depth of backfill soil, the earth pressure load gradually increased. The measured earth pressure was greater than the at-rest earth pressure and the active earth pressure, but less than the passive earth pressure. The stress test data of the internal steel plate in the silo wall are shown in Fig.3b. As the height of the silo wall increased, the circumferential stress of the internal steel plate also increased. The average circumferential stresses of the internal steel plate at 0.45 m, 1.70 m, and 2.85 m were -5.06 MPa, -6.78 MPa, and -8.72 MPa, respectively (negative values indicate compression, the same below). With the increase in the angle of the silo wall, the stress values of the internal steel plate at the same height generally did not differ significantly. Along the circumferential direction of the silo wall from 0° to 30°, the stress first increased and then decreased. Analysis of the stress variation pattern revealed that from 0° to 30°, the constraint of the joint on the internal steel plate first weakened and then strengthened, resulting in the circumferential stress of the internal steel plate first increasing and then decreasing.

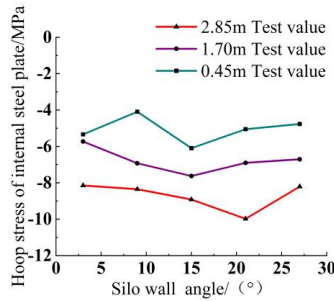
The circumferential stress of the hoop reinforcement inside the silo wall is shown in Fig.3c. The stress variation trend of the hoop reinforcement at the three heights was generally similar to that of the internal steel plate. As the height of the silo wall increased, the circumferential stress of the hoop reinforcement gradually increased. Along the angle direction of the silo wall, the circumferential stress of the hoop reinforcement also generally showed a trend of first increasing and then decreasing with the change in the angle of the silo wall. The average circumferential stresses of the hoop reinforcement at 0.45 m, 1.70 m, and 2.85 m were -5.47 MPa, -6.79 MPa, and -8.46 MPa, respectively.

The results indicate that at the same height, the circumferential compressive stress of the internal steel plate and the hoop reinforcement in the silo wall were not significantly different. Along the circumferential direction of the silo wall, the stress first increased and then decreased. The circumferential stress was relatively lower near the joint and higher at the middle position.

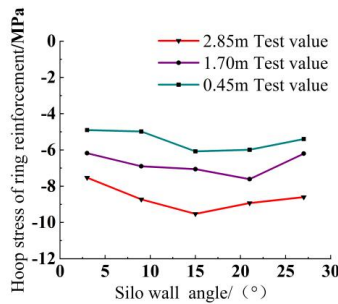


Note: P<sub>1</sub> indicates the static earth pressure, P<sub>2</sub> indicates the passive earth pressure, P<sub>3</sub> indicates the active earth pressure, P<sub>4</sub> indicates the measured earth pressure, P<sub>5</sub> indicates the fitted earth pressure.

a. Earth pressure comparison.



b. Hoop stress test value of internal steel plate.



c. Hoop stress test value of ring reinforcement

Fig. 3. Measurement point data chart.

### 3 Finite Element Model Validation

#### 3.1 Establishment of Finite Element Model

A finite element numerical model corresponding to the dimensions and material parameters of the actual underground silo was constructed using the ABAQUS software. The material attributes of each component are delineated in Table 1. The internal steel plate, external waterproof steel plate, and similar components were modeled utilizing shell elements (S4R). Reinforcement bars were instantiated with link elements (T3D2), while other components were established using solid elements (C3D8R). As depicted in Fig.4, the model predominantly employed a hexahedral element structured mesh to discretize each component. The earth pressure load on the exterior of the silo wall was applied in accordance with the fitted curve derived from the measured earth pressure. The fitting formula is:  $P = -0.000026 \times Z + 0.24$ ,  $P$  is the side pressure of the silo wall corresponding to different heights, MPa;  $Z$  is the backfill height, mm. The rebar mesh was embedded within the silo wall concrete. The connections between the interna steel plate and the silo wall concrete, between the silo bottom and top and the silo wall, and among the components at the joint were all modeled using tie constraints. The silo bottom plate was considered as a fixed end, with translational and rotational constraints applied in the X, Y, and Z directions.

**Table 1.** Material property sheet.

material	density/t·mm <sup>-3</sup>	Elastic modulus/MPa	Poisson's ratio
Steel plate	$7.8 \times 10^{-9}$	$2.06 \times 10^5$	0.3
Concrete	$2.8 \times 10^{-9}$	$3.25 \times 10^4$	0.2
Rebar	$7.8 \times 10^{-9}$	$2.00 \times 10^5$	0.3

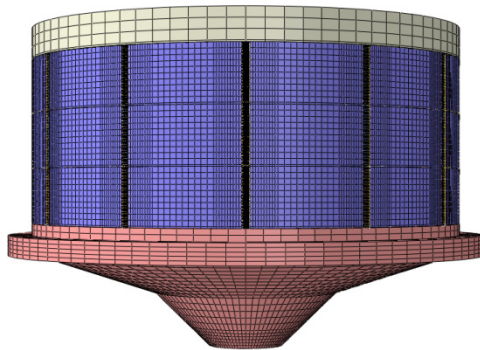
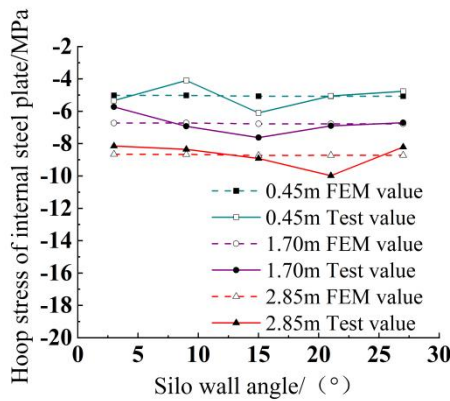


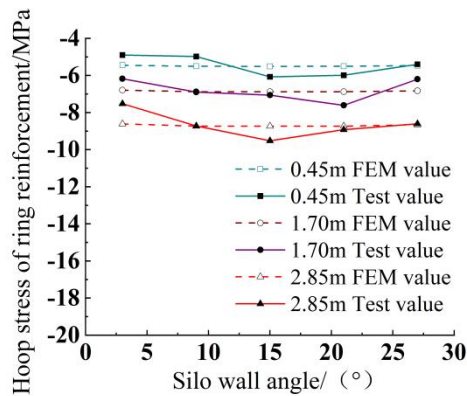
**Fig. 4.** Finite element geometric model and meshing diagram.

### 3.2 Finite Element Model Validation

To validate the effectiveness of the finite element model, the experimental data from the silo wall measurement points were compared with the corresponding finite element data. As shown in Fig.5, the circumferential stress values of the internal steel plate and hoop reinforcement in the finite element model varied relatively smoothly along the angle direction of the silo wall. The experimental values fluctuated around the simulated values, showing an overall trend of first decreasing and then increasing, with good agreement. The average errors between the simulated and experimental values of the circumferential stress for the internal steel plate and hoop reinforcement were 7.84% and 6.56%, respectively, which demonstrate the validity of the constraints and load application in the finite element model of the underground silo.



a Comparison of hoop stress of internal steel plate.



b Comparison of hoop stress of ring reinforcement.

Fig. 5. Comparison of hoop stress test value and finite element calculation value.

## 4 Finite Element Parameter Analysis

The underground silo is a composite structure of cylindrical shells, with the silo wall being jointly restrained by the silo bottom and top. Under the action of earth pressure load, the primary internal force in the silo wall is the circumferential stress. According to relevant studies<sup>[17]</sup> on the selection of lateral earth pressure for silo walls, to fully ensure the safety and reliability of the structure, and in combination with the experimental results of this paper and relevant references, the passive earth pressure is adopted for the analysis and calculation of the underground silo in this section. To further investigate the variation pattern of the internal forces in the silo wall, a numerical simulation method was employed to conduct a parametric analysis of this underground silo. Finite element models were established by taking different values for design parameters such as concrete strength, external waterproof steel plate thickness, and internal steel plate thickness. The values of the design parameters and the main results are shown in Table 2. The parametric analysis was conducted to study the influence of changes in each parameter on the circumferential stress and radial displacement of the silo wall.

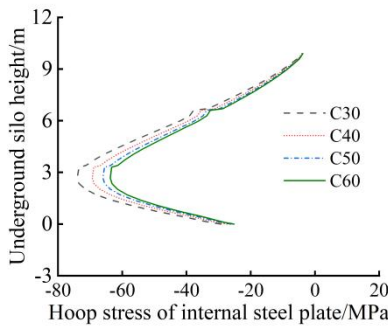
**Table 2.** Analysis parameters and main results of finite element model.

Finite element model	Concrete strength/MPa	Thickness of external waterproof steel plate/mm	Thickness of internal steel plate/mm	Maximum circumferential stress of concrete of silo wall/MPa	Maximum circumferential stress of internal steel plate of silo wall/MPa	Maximum displacement of silo wall/mm
FSC-C30	30			-12.25	-74.02	-4.77
FSC-C40	40			-12.42	-69.34	-4.47
FSC-C50	50	16	10	-12.55	-66.01	-4.26
FSC-C60	60			-12.63	-63.71	-4.11
FSC-J10		10		-12.45	-69.21	-4.50
FSC-J12		12		-12.44	-69.26	-4.49
FSC-J14	40	14	10	-12.43	-69.31	-4.48
FSC-J16		16		-12.42	-69.34	-4.47
FSC-I6			6	-13.25	-74.31	-4.77
FSC-I8			8	-12.82	-71.76	-4.61
FSC-I10	40	16	10	-12.42	-69.34	-4.47
FSC-I12			12	-12.05	-67.12	-4.34

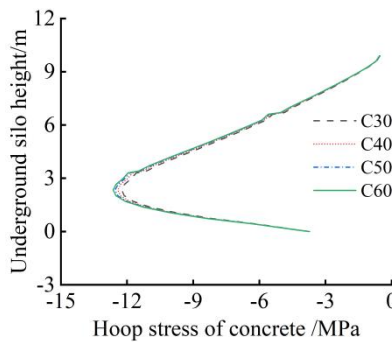
Note: FSC-C indicates the model that changes the elastic modulus of concrete. FSC-J indicates the model that changes the external waterproof steel plate thickness. FSC-I indicates the model that changes the internal steel plate thickness.

### 4.1 Influence of Concrete Strength on Internal Force of Silo Wall

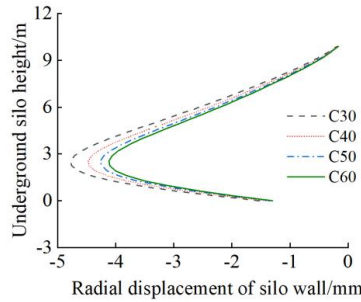
As the concrete strength increases, the circumferential stress in the silo wall decreases. As shown in Fig.6a and Fig.6b, compared with the use of concrete with a strength of C30, the maximum circumferential stress of the internal steel plate in the underground silo using concrete with strengths of C40, C50, and C60 decreases by 6.32%, 10.82%, and 12.93%, respectively. However, changes in concrete strength have a relatively small effect on the circumferential stress of the concrete along the height of the silo wall. As shown in Fig.6c, the radial displacement of the silo wall decreases significantly with the increase in concrete strength. The increase in concrete grade enhances the elastic modulus of the concrete. Therefore, the increase in concrete strength can not only enhance the load-carrying capacity of the silo wall but also reduce the radial displacement of the silo wall. Thus, in actual engineering design, it is recommended to appropriately increase the concrete strength. However, the strength should not be too high. Concrete with a strength grade of C40 to C50 is recommended.



a Effect of concrete strength on hoop stress of internal steel plate



b. Effect of concrete strength on hoop stress of concrete.

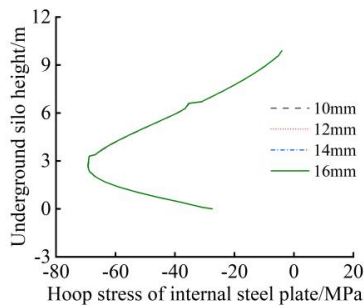


c. Effect of concrete strength on radial displacement of silo wall.

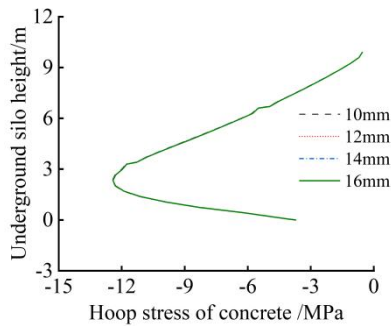
Fig. 6. Influence of concrete strength on the internal forces within silo wall.

### 4.2 Influence of External Waterproof Steel Plate Thickness on Internal Force of Silo Wall

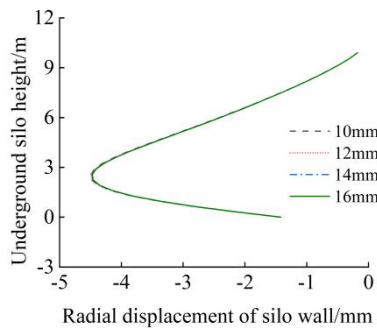
Based on the finite element model of the prototype test silo, only the thickness of the external waterproof steel plate was changed. The effects on the circumferential stress and displacement of the silo wall are shown in Fig.7a, 7b, and 7c. The thickness of the external waterproof steel plate has a relatively small impact on the circumferential stress of the internal steel plate and concrete, as well as the radial displacement of the silo wall. As the thickness of the external waterproof steel plate increases, the influence on the circumferential stress of the internal steel plate and concrete, and the radial displacement is minimal, with changes not exceeding 0.24%, 0.18%, and 0.67%, respectively. The reason is that the circumferential stress of the silo wall is mainly borne by the internal steel plate and concrete, while the external waterproof steel plate primarily serves a waterproofing function. Therefore, in the design of underground silos, it is recommended to use a relatively thin external waterproof steel plate, but not too thin. Considering structural construction and economic rationality, a 10 mm thick internal waterproof steel plate is suggested.



a Effect of external waterproof steel plate thickness on hoop stress of internal steel plate.



b Effect of external waterproof steel plate thickness on hoop stress of concrete.

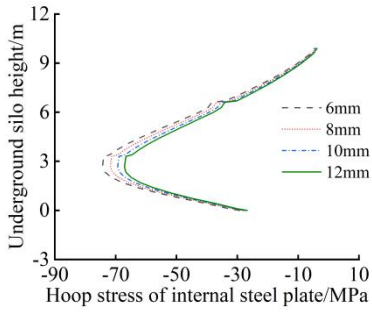


c. Effect of external waterproof steel plate thickness on radial displacement of silo wall.

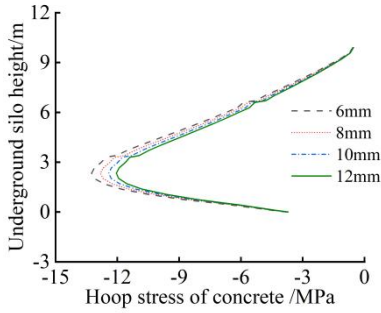
Fig. 7. Influence of external waterproof steel plate thickness on internal force of silo wall.

### 4.3 Influence of Thickness of Internal Steel Plate on Internal Force of Silo Wall

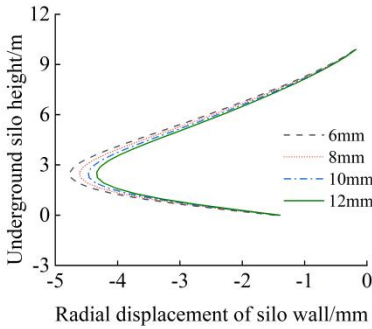
As shown in Fig.8a and 8b, the circumferential stress of the silo wall decreases significantly with the increase in the thickness of the internal steel plate. Compared with the FEM-I6 model, the maximum circumferential stress of the internal steel plate in the FEM-I8, FEM-I10, and FEM-I2 models decreases by 3.43%, 6.69%, and 9.68%, respectively. It can also be observed that the circumferential stress of the silo wall concrete is reduced to a certain extent. Increasing the thickness of the internal steel plate enhances the overall stiffness of the silo wall, which can better distribute and resist the external earth pressure load, thereby reducing the circumferential stress of the silo wall. As shown in Fig.8c, with the increase in the stiffness of the silo wall, the deformation of the silo wall also decreases. Therefore, from the perspective of underground silo design, the thickness of the internal steel plate can be increased to reduce the circumferential stress and displacement of the silo wall. Considering structural construction and economic rationality, a 10mm thick internal steel plate is recommended.



a Effect of internal steel plate thickness on hoop stress of internal steel plate.



b Effect of internal steel plate thickness on hoop stress of concrete.



c. Effect of internal steel plate thickness on radial displacement of silo wall.

**Fig. 8.** Influence of thickness of internal steel plate on internal force of silo wall.

## 5 Discussion and Limitation

The study focused solely on the earth pressure under the empty silo condition. However, actual operating conditions are complex and variable. The combined effects of various loads such as the lateral pressure of grain and the groundwater pressure when the silo is full have not been thoroughly investigated. This limits the study's ability to reflect the true stress conditions of underground silos. The parametric analysis only covered some key design parameters such as concrete strength, external waterproof steel plate thickness, and internal steel plate thickness. Other factors that may affect the performance of the silo wall were not considered, restricting the breadth of the research. Future research could expand to the mechanical performance of the silo wall under various complex load condition combinations, taking into account factors such as the lateral pressure of grain and groundwater pressure to construct a more realistic stress model.

## 6 Conclusions

This paper takes a steel-plate–concrete composite underground silo as the research object. The distribution pattern of the circumferential stress in the silo wall under the action of earth pressure in the most unfavorable condition (empty silo) was analyzed through experiments. A corresponding finite element model of the prefabricated underground silo was established, and the experimental results were compared and verified with the finite element model data. Parametric analysis was also conducted on important component parameters of the underground silo. The main conclusions are as follows:

(1) Under the action of earth pressure load, the circumferential stress at the same height along the circumferential direction of the silo wall does not differ significantly, and the peak compressive stress appears at the middle position of a single silo wall. The circumferential stress of the measurement points on the silo wall increases gradually along the height of the silo.

(2) The finite element analysis results are in good agreement with the field test data. Under the action of backfill load, the average errors between the experimental values and the finite element simulation values of the circumferential stress of the internal steel plate and hoop reinforcement are 7.84% and 6.56%, respectively, which verifies the validity of the finite element model.

(3) Through parametric analysis, the effects of key design parameters such as concrete strength, external waterproof steel plate thickness, and internal steel plate thickness on the distribution of circumferential stress in the silo wall were investigated. Concrete strength and internal steel plate thickness have a significant impact on the circumferential stress in the silo wall. Increasing the concrete strength can significantly reduce the circumferential stress of the internal steel plate and the maximum radial displacement of the silo wall. In contrast, increasing the thickness of the external waterproof steel plate has a negligible effect on the circumferential stress and radial displacement of the silo wall. Increasing the thickness of the internal steel plate can significantly

reduce the circumferential stress of the silo wall concrete and internal steel plate, as well as the radial displacement of the silo wall.

## References

1. WU Yuling, ZHANG Pei, YU Yiyi, et al. "Progress Review on and Prospects for Non-grain Cultivated Land in China from the Perspective of Food Security," *China Land Science*: 35(09): 116-124, 2021.
2. PRATS G. "Underground silo storage during the Late Bronze and Early Iron Ages: An approach to the different realities of the Northeast of the Iberian Peninsula," *Journal of Archaeological Science: Reports*: 31: 102272, 2020.
3. VALLS A, GARCÍA F, RAMÍREZ M, et al. "Understanding subterranean grain storage heritage in the Mediterranean region: The Valencian silos (Spain)," *Tunnelling and Underground Space Technology*: 50: 178-188, 2015.
4. WANG Zhenqing, ChUAI Jun, LIU Yongchao, et al. "Current Situation and New Progresses of Structure Design of Underground Silos," *Journal of Henan University of Technology (Natural Science Edition)*: 40(5): 132-138, 2019.
5. PAN Y, FANG H, LI B, et al. "Stability analysis and full-scale test of a new recyclable supporting structure for underground ecological granaries," *Engineering Structures* 192: 205-219, 2019. doi:10.1016/j.engstruct.2019.04.087.
6. Liu Haiyan, Meng Weixin, Wang Zhenqing, et al. "Buoyancy early warning of underground granary with "2:8 lime soil" backfilling," *Transactions of the Chinese Society of Agricultural Engineering*: 35(11): 299-305, 2019.
7. ZHANG Q, OUYANG L, WANG Z, et al. "Buoyancy Reduction Coefficients for Underground Silos in Sand and Clay," *Indian Geotechnical Journal*: 49: 216-223, 2019.
8. ZHANG Hao, MENG Qingting, TAO Yuanqing. "Experiment on water pressure resistance of plastic-concrete waterproof system of underground granary," *Transactions of the Chinese Society of Agricultural Engineering*: 36(21): 292-299, 2020.
9. ZHANG H, HAN K, YANG J, et al. "Experimental and Numerical Investigation of Plastic-Concrete Waterproof Walls of an Underground Granary Subject to Combined Bending Moment and Water Pressure," *Buildings* 12(7): 893, 2022. doi:10.3390/buildings12070893.
10. ZHANG H, WANG H, ZHOU Y, et al. "Waterproofing performance of polypropylene-concrete wall of underground silo under combined compressive stress and water pressure," *Helvion* 8(12), 2022. doi:10.1016/j.helivon.2022.e12074.
11. QINGZHANG Z, ZHILONG H, HAO Z, et al. "Experimental study on resisted water pressure for connecting welds of polypropylene plastic plates in underground silos," *Plastics, Rubber and Composites* 51(6): 316-324, 2022. doi:10.1080/14658011.2021.1989928.
12. ZHANG H, WANG H, YANG J, et al. "A novel vertical waterproofing joint with trapezoidal steel plate connections for steel-concrete underground silos: Bending test and numerical simulation," *Tunnelling and Underground Space Technology* 137: 105150, 2023. doi:10.1016/j.tust.2023.105150.
13. CHUAI J, HOU Z, WANG Z, et al. "Mechanical properties of the vertical joints of prefabricated underground silo steel plate concrete wall," *Advances in Civil Engineering* 2020(1): 6643811, 2020. doi:10.1155/2020/6643811.
14. WANG Zhenqing, CHUAI Jun, WANG Lumin, et al. "Finite element analysis on mechanical properties of joint in precast steel plate-concrete composite wall of underground granary," *Transactions of the Chinese Society of Agricultural Engineering*: 35(24): 298-306, 2019.

15. KIM S, KIM K. "Numerical parametric studies on the stress distribution in rocks around underground silo," *Applied Sciences* 12(3): 1613, 2022. doi:10.3390/app12031613.
16. KIM S, KIM K. "Numerical Study of Structural Behavior of Underground Silo Structures for Low-and-Intermediate-level Radioactive Waste Disposal Facility," *Journal of the Computational Structural Engineering Institute of Korea* 35(3): 183-190, 2022. doi:10.7734/COSEIK.2022.35.3.183.
17. XIONG Xiaoli, JIN Libing, WANG Zhenqing. "Earth Pressure and Bearing Capacity Analysis on the Wall of Reinforced Concrete Underground Granary," *Journal of Basic Science and Engineering*: 24(1): 103-114, 2016.

**Open Access** This chapter is licensed under the terms of the Creative Commons Attribution-NonCommercial 4.0 International License (<http://creativecommons.org/licenses/by-nc/4.0/>), which permits any noncommercial use, sharing, adaptation, distribution and reproduction in any medium or format, as long as you give appropriate credit to the original author(s) and the source, provide a link to the Creative Commons license and indicate if changes were made.

The images or other third party material in this chapter are included in the chapter's Creative Commons license, unless indicated otherwise in a credit line to the material. If material is not included in the chapter's Creative Commons license and your intended use is not permitted by statutory regulation or exceeds the permitted use, you will need to obtain permission directly from the copyright holder.

